Sigma J Eng & Nat Sci 36 (4), 2018, 977-992

Sigma Journal of Engineering and Natural Sciences
Sigma Mühendislik ve Fen Bilimleri Dergisi

Research Article

COMPARISON OF FEM SOLUTION WITH ANALYTICAL SOLUTION OF CONTINUOUS AND DISCONTINUOUS CONTACT PROBLEM

Yusuf KAYA*[1], Alper POLAT[2], Talat Şükrü ÖZŞAHİN[3]

[1]*Gumuhane University, Civil Engineering Department, GUMUSHANE;* ORCID:0000-0002-1894-1146
[2]*Munzur University, Construction Technology Department, TUNCELI;* ORCID:0000-0002-6368-5276
[3]*Karadeniz Technical University, Civil Engineering Department, TRABZON;* ORCID:0000-0002-1179-6556

Received: 17.04.2018 Accepted: 29.06.2018

ABSTRACT

The continuous and discontinuous contact problem of a homogeneous layer loaded with three rigid flat blocks and resting on the elastic semi-infinite plane was investigated in this study by using the finite element method (FEM). All surfaces are assumed to be frictionless. The homogenous layer was loaded by means of three rigid flat blocks whose external loads are Q and P (per unit thickness in *z* direction). Two dimensional finite element analysis of the problem was performed using ANSYS package program. Analyzes were performed for loading conditions which are *Q=P*, *Q=2P*, *Q=4P*, *Q=8P* and *Q=10P*, and different values of block widths, distances between blocks and shear modulus. The initial separation loads and initial separation distances $(\lambda_{cr}, \chi_{cr})$ between the homogeneous layer and the elastic semi-infinite plane were determined for continuous contact condition. The length of the separation zone was obtained for discontinuous contact condition. In addition to these, normal stress distributions between the layer and the semi-infinite plane were determined for continuous and discontinuous contact conditions. As a result of the study, the analytical results, and the results of the finite element method were shown by comparing as graphs and tables.
Keywords: Continuous contact, discontinuous contact, homogenous layer, finite element method.

1. INTRODUCTION

The contact problem is one of the main problems of elasticity. Since many of building elements and system elements are in contact with each other, the contact issue has been involved widely in many engineering fields. The contact issue was discussed firstly by Heinrich Hertz in 1882, and an increase was observed in the studies on contact problems along with the complex variables method developed by Muskhelishvili and the using of integral transformation techniques in the theory of elasticity by Sneddon [1-3]. A number of researchers have discussed contact problems such as continuous and discontinuous contact problem [4-6], contact and crack problem [7-9], frictional and moving contact problem [10-12] and the receding contact problem [13-16] until today.

Highly complex mathematical analyzes of idealized systems must be performed in order to solve the contact problem analytically. These solutions can be applied to many problems as partly

* Corresponding Author: e-mail: yusufkaya@gumushane.edu.tr, tel: (456) 233 10 00 / 1632

or completely successful depending on how the actual geometry of the problem and the loading condition close to the mathematical modeling. For this reason, numerical methods which give solution in acceptable approximation such as finite elements, finite differences and boundary elements are used to solve engineering problems [17]. The finite element method (FEM), which looks for a solution by making complex engineering problem simpler, has become one of the preferred solution methods in recent years. Firstly, Chan and Tuba (1971) developed a solution to the plane contact problem of elastic bodies by using the finite element method. Afterwards, a number of researchers solved the frictional contact problem [18-20], the receding contact problem [21-23], continuous and discontinuous contact problem [24-25] by using the finite element method. Birinci et al., solved continuous and discontinuous contact problem on a layer loaded with spread load in analytically and numerically in the study that was conducted in 2015 [26]. Polat et al., solved the continuous contact problem of the homogeneous layer loaded with 2 rigid blocks and resting on elastic half plane by using finite element method in the study that they carried out in 2017 [27]. Then they compared the results with the analytical solution.

When examining the previous studies, it is seen that the studies on contact problems in which the mass forces are taken into consideration by using the finite element method are few. The continuous and discontinuous contact problem on a homogeneous layer loaded with three different rigid blocks with different external loads and resting on elastic half-planes was solved in this study by using Finite Elements Method (FEM), and the results were compared with the analytical results of Ozşahin and Taskiner's study (2013) [5]. The initial separation loads and distances, the stresses under the block and the normal stresses along the x-axis between the homogeneous layer and the elastic plane for different load ratios were determined, and the starting and end points of the separation for different load ratios and shear modulus were also determined in case of discontinuous contact. In addition, the stress distribution between the homogeneous layer and the elastic semi-infinite plane for continuous and discontinuous contact conditions was determined by both solution methods. The results that were obtained are given as comparative graphs and tables.

2. DEFINITION OF PROBLEM

The continuous contact problem of the homogeneous layer at the (h) height and resting on elastic half-plane is solved analytically with the help of elasticity theory and integral transformation techniques [5]. The external loads Q, P and Q are transferred to the layers by three rigid blocks with different. All surfaces in the problem are frictionless. In addition, the rigid blocks are in contact with the homogeneous layer at intervals of (-c, -d), (-a, a) and (c, d). The mass force of the layer is considered as ρgh in the solution. Where ρ is the density of the homogeneous layer, g is gravitational acceleration.

The layer and the rigid plane extend along the x-axis in the range of $(-\infty, +\infty)$. The x=0 plane is plane of symmetry according to external loads and geometry. Therefore, it is enough to take half of the medium in the analytical solution of the problem. In addition, the thickness in the z-axis direction was taken as unit since the problem would be examined for state of plane.

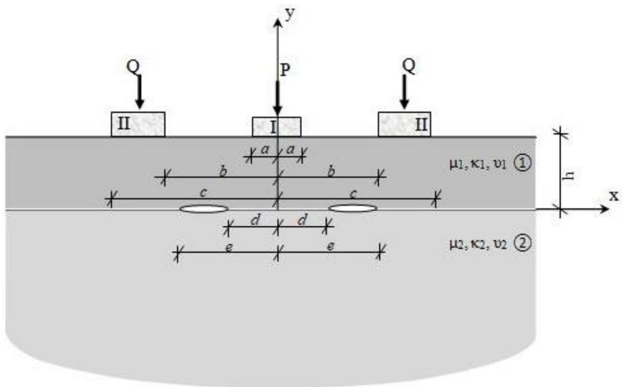

Figure 1. Elastic layer re sting on an elastic half plane loaded by means of three rigid flat blocks.

3. BOUNDARY CONDITIONS OF CONTINUOUS CONTACT PROBLEM, AND INTEGRAL EQUATION

While the and represent displacement components and and represent stress components, the boundary conditions of the problem can be written as follows according to the axis group in Figure 1:

$$\sigma_{y_1}(x,0)=\begin{cases}-P(x) & 0<x<a \\ -Q(x) & b<x<c \\ 0 & a<x<b,\ c<x<\infty\end{cases} \tag{1a}$$

$$\tau_{xy_1}(x,h)=0 \qquad 0<x<\infty \tag{1b}$$

$$\tau_{xy_1}(x,0)=0 \qquad 0<x<\infty \tag{1c}$$

$$\tau_{xy_2}(x,0)=0 \qquad 0<x<\infty \tag{1d}$$

$$\sigma_{y_1}(x,0)=\sigma_{y_2}(x,0) \qquad 0<x<\infty \tag{1e}$$

$$\frac{\partial}{\partial x}\left[v_2(x,0)-v_1(x,0)\right]=0 \qquad 0<x<\infty \tag{1f}$$

$$\frac{\partial}{\partial x}\left[v_1(x,h)\right]=0 \qquad 0<x<a \tag{1g}$$

$$\frac{\partial}{\partial x}\left[v_1(x,h)\right]=0 \qquad b<x<c \tag{1h}$$

The P (x) and the Q (x) which are in (1a) numbered statement are contact stresses between rigid blocks and homogeneous layers.
Equilibrium conditions of problem;

$$\int_0^a P(x)dx=\frac{P}{2} \quad \text{(a)}$$

$$\int_b^c Q(x)dx=Q \quad \text{(b)} \tag{2a-b}$$

The unknowns A, B, C, D, E and F are obtained depending on Q and P by substituting the boundary conditions in (1a-f) statements to their place in the stress and displacement statements. The following singular integral equations for P (x) and Q (x) can be obtained by using (1g) and (1h), after some simple operations: [28]

$$-\frac{1}{\pi\mu_1}\int_0^a\left[k_1(x,t)+\frac{(1+\kappa_1)}{4}\left(\frac{1}{t-x}+\frac{1}{t+x}\right)\right]P(t)dt$$
$$-\frac{1}{\pi\mu_1}\int_c^d\left[k_1(x,t)+\frac{(1+\kappa_1)}{4}\left(\frac{1}{t-x}+\frac{1}{t+x}\right)\right]Q(t)dt=0,\quad 0<x<a, \tag{3a}$$

$$-\frac{1}{\pi\mu_1}\int_0^a\left[k_1(x,t)+\frac{(1+\kappa_1)}{4}\left(\frac{1}{t-x}+\frac{1}{t+x}\right)\right]P(t)dt$$
$$-\frac{1}{\pi\mu_1}\int_c^d\left[k_1(x,t)+\frac{(1+\kappa_1)}{4}\left(\frac{1}{t-x}+\frac{1}{t+x}\right)\right]Q(t)dt=0,\quad b<x<c, \tag{3b}$$

Where, $k_1(x,t)$, is the Fredholm Kernel of the singular integral equations. μ_i and κ_i *(i=1,2)* in the equations are elastic constants.

κ is a material constant (Kolosov's Constant) and is known as the $\kappa = 3-4\upsilon$ in plane of strain, $\kappa = \frac{(3-\upsilon)}{(1+\upsilon)}$ in plane stress. υ_i is the Poisson's ratio and is taken between 0.15~0.35 in this study.

$$k_1(x,t)=\int_0^\infty\left\{\left\{\frac{\alpha^3}{8(1+\kappa_1)}\left[(1+\kappa_2)\left[-e^{-4\alpha h}+4\alpha he^{-2\alpha h}+1\right]+\frac{\mu_2}{\mu_1(1+\kappa_1)}\left[e^{-4\alpha h}-2e^{-2\alpha h}+1\right]\right]\right\}\Big/\Delta\right.$$
$$\left.-\frac{(1+\kappa_1)}{4}\right\}\times\{\sin\alpha(t+x)-\sin\alpha(t-x)\}d\alpha, \tag{4}$$

Where Δ is:

$$\Delta=\alpha^3\left\{(1+\kappa_2)\left[-e^{-4\alpha h}+e^{-2\alpha h}(2+4\alpha^2h^2)-2\right]+\frac{\mu_2}{\mu_1(1+\kappa_1)}\left[e^{-4\alpha h}+4\alpha he^{-2\alpha h}-2\right]\right\} \tag{5}$$

Also the stress relation between the homogeneous layer and the elastic half-plane is obtained as follows:

$$\sigma_{y_1}(x,0)=-\rho_1 gh-\frac{1}{\pi}\int_0^a k_2(x,t)P(t)dt-\frac{1}{\pi}\int_b^c k_2(x,t)Q(t)dt,\qquad 0<x<\infty \tag{6}$$

Where $k_2(x,t)$ is:

$$k_2(x,t)=\int_0^\infty\left\{\alpha^3\frac{\mu_2}{\mu_1(1+\kappa_1)}\left[e^{-3\alpha h}(-1+\alpha h)+e^{-\alpha h}(1+\alpha h)\right]\right\}\Big/\Delta\times\{\cos\alpha(t+x)+\cos\alpha(t-x)\}d\alpha \tag{7}$$

The following dimensionless quantities are defined to facilitate the numerical solution of the integral equation:

$$x_1=ar_1,\quad t_1=as_1,\quad x_2=\frac{c-b}{2}r_2+\frac{c+b}{2},\quad t_2=\frac{c-b}{2}s_2+\frac{c+b}{2},\quad g_1(s_1)=P(as_1)\big/P/h,$$
$$g_2(s_2)=Q\left(\frac{c-b}{2}s_2+\frac{c+b}{2}\right)\Big/P/h,\qquad \alpha=wh\qquad \lambda=\frac{P}{\rho_1 gh^2}. \tag{8a-h}$$

λ indicates the load factor. In case the λ load factor reaches a certain critical value, separation occurs between the layer and the elastic half-plane, and the problem becomes a discontinuous contact problem. The distance where the initial separation occurs is named (χ_{cr}).

In case the load reaches the critical load, the load factor formula is as follows:

$$\lambda_{cr} = \frac{P_{cr}}{\rho_1 g h^2} \tag{9}$$

Other equations can be seen in the ref [5].

4. BOUNDARY CONDITIONS OF THE DISCONTINUOUS CONTACT PROBLEM, AND THE INTEGRAL EQUATION

In case the load factor is larger than the critical load factor (λ> λcr), it will be seperation between the homogeneous layer and the elastic half plane as shown in Figure 1. It is assumed that the separation zone is in the range of d <x <e, and on the point of y = -h. The boundary conditions for discontinuous contact can be written as follows according to the axis group in Figure 1:

$$\sigma_{y_1}(x,0) = \begin{Bmatrix} -P(x) & 0<x<a \\ -Q(x) & b<x<c \\ 0 & a<x<b,\ c<x<\infty \end{Bmatrix} \tag{10a}$$

$$\tau_{xy_1}(x,h) = 0 \qquad 0<x<\infty \tag{10b}$$

$$\tau_{xy_1}(x,0) = 0 \qquad 0<x<\infty \tag{10c}$$

$$\tau_{xy_2}(x,0) = 0 \qquad 0<x<\infty \tag{10d}$$

$$\sigma_{y_1}(x,0) = \sigma_{y_2}(x,0) \qquad 0<x<\infty \tag{10e}$$

$$\frac{\partial}{\partial x}\left[v_2(x,0) - v_1(x,0)\right] = \begin{Bmatrix} \varphi(x) & d<x<e \\ 0 & 0<x<d,\ e<x<\infty \end{Bmatrix} \tag{10f}$$

$$\sigma_{y_1}(x,0) = \sigma_{y_2}(x,0) = 0 \qquad d<x<e \tag{10g}$$

$$\frac{\partial}{\partial x}\left[v_1(x,h)\right] = 0 \qquad 0<x<a \tag{10h}$$

$$\frac{\partial}{\partial x}\left[v_1(x,h)\right] = 0 \qquad b<x<c \tag{10i}$$

Where, d and e are unknowns, and they are a function of the load factor (λ). The φ(x) which is in the equation (10f) is an unknown function, and the the single-valuedness condition can be written as follows:

$$\int_d^e \varphi(x)dx = 0 \tag{11}$$

The unknowns A, B, C, D, E and F are obtained by substituting the boundary conditions in (10a-f) statements to their place in the stress and displacement statements. The following singular integral equations for the P (x) Q (x) and φ (x) can be obtained by using (10h) and (10i), after some simple operations [28]:

$$-\frac{1}{\pi\mu_1}\int_0^a\left[k_1(x,t)+\frac{(1+\kappa_1)}{4}\left(\frac{1}{t-x}-\frac{1}{t+x}\right)\right]P(t)dt\ -\frac{1}{\pi\mu_1}\int_c^d\left[k_1(x,t)+\frac{(1+\kappa_1)}{4}\left(\frac{1}{t-x}-\frac{1}{t+x}\right)\right]Q(t)dt$$
$$+\frac{1}{\pi}\int_d^e k_2(x,t)\varphi(t)dt=0\,,\quad 0<x<a\,, \tag{12a}$$

$$-\frac{1}{\pi\mu_1}\int_0^a\left[k_1(x,t)+\frac{(1+\kappa_1)}{4}\left(\frac{1}{t-x}-\frac{1}{t+x}\right)\right]P(t)dt\ -\frac{1}{\pi\mu_1}\int_c^d\left[k_1(x,t)+\frac{(1+\kappa_1)}{4}\left(\frac{1}{t-x}-\frac{1}{t+x}\right)\right]Q(t)dt\,,$$
$$+\frac{1}{\pi}\int_d^e k_2(x,t)\varphi(t)dt=0 \qquad b<x<c\,, \tag{12b}$$

$$\frac{1}{\pi}\int_0^a k_2(x,t)P(t)dt+\frac{1}{\pi}\int_b^c k_2(x,t)Q(t)dt$$
$$-\frac{\mu_1}{\pi}\int_d^e\left[k_3(x,t)-\frac{4\mu_2/\mu_1}{(1+\kappa_2)+\mu_2/\mu_1(1+\kappa_1)}\left(\frac{1}{t-x}+\frac{1}{t+x}\right)\right]\varphi(t)dt-\rho_1 gh=0 \tag{12c}$$

Where, $k_1(x,t)$ and $k_2(x,t)$ are as given in the equations of (7) and (10). $k_3(x,t)$ is obtained as follows:

$$k_3(x,t)=\int_0^\infty\left\{\left\{-\frac{2\alpha^3\mu_2}{\mu_1}\left[\left[e^{-2\alpha h}(4\alpha^2h^2+2)-e^{-4\alpha h}-1\right]\times(\Delta)^{-1}+\frac{4\mu_2/\mu_1}{(1+\kappa_2)+\mu_2/\mu_1(1+\kappa_1)}\right]\right\}$$
$$\times\{\sin\alpha(t+x)+\sin\alpha(t-x)\}\,d\alpha\,, \tag{13}$$

Δ in this case is as in equation (8).

The following dimensionless quantities are defined in addition to the equations of (8a-h) in order to facilitate the numerical solution of the integral equation:

$$x_3=\frac{e-d}{2}r_3+\frac{e+d}{2}\,,\ t_3=\frac{e-d}{2}s_3+\frac{e+d}{2},\ \ g_3(s_3)=\frac{\mu_1\varphi\big(((e-d)/2)s_3+(e+d)/2\big)}{P/h} \tag{14a-c}$$

Other equations can be seen in the ref [5].

5. SOLUTION WITH FINITE ELEMENT METHOD

Finite element method (FEM) is a numerical method which is used to find approximate solutions of complex problems. It is sought for solutions in this method by reducing complicated engineering geometries to simple geometries in finite number. The problem is made simpler in this process called mesh by making mathematical operation on a number of small sub-parts instead of the whole problem. Although it is important in terms of approaching the exact solution of a large number of mesh problems, it can be seen as a disadvantage since it increases the solution time. The finite element model and analysis of problem was performed by using ANSYS Mechanical APDL Product Launcher (2015) package program [29]. This software runs finite element analysis by using various numerical solutions together with the dividing into the appropriate networks and error control [30]. The problem was modelled symmetrically and the weight was taken into account, but the frictional force is neglected on all surfaces. Linear, elastic and isotropic materials were used in all parts of the model. Determination of the element type is important in terms of getting correct results in solving the problem. PLANE183 with 8 nodes is used as the element type because this study is static and 2 dimensional plane stress problem. PLANE 183 has degrees of freedom in the x and y directions at each node and has no freedom of rotation. In addition, surface-to-surface contact model was used in order to provide a solution in case the nodes did not overlay while modeling in the study.

When the contact pair was formed, the 2D target surface was defined with the TARGE 169 element and the two-dimensional contact surface with the CONTA 172 element. A surface with large elasticity modulus is selected as the target. TARGE 169 and CONTA 172 are elements with three nodal points, and nodes correspond to the nodes on the surface of PLANE 183 element. A rectangle was chosen as the mesh geometry to divide elements into networks. There are various contact algorithms in ANSYS depending on the problem type. The Augmented Lagrangian Method, which uses the total potential energy theorem as the contact algorithm and gives better and faster results than the other algorithms, was preferred in this study. The finite element model of the problem is given in Figure 2, the flow diagram belonging to finite element model is given in Figure 3:

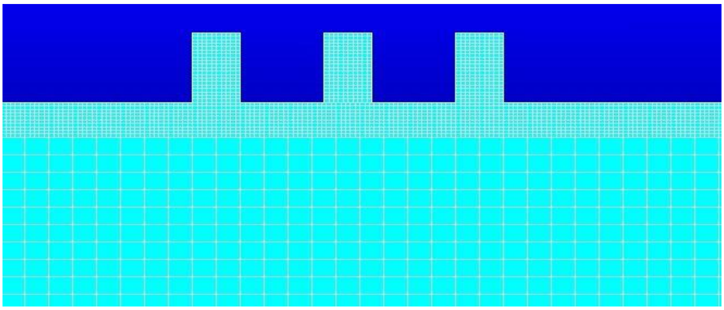

Figure 2. FEM modeling of the contact problem before analysis

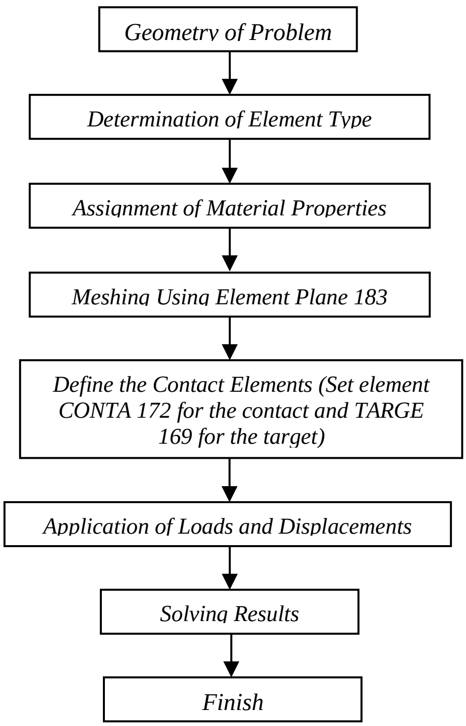

Figure 3. The details of the FEM procedure

6. RESULTS AND DISCUSSION

The analysis of continuous and discontinuous contact problem was analyzed in this study by using Finite Element Method (FEM), and the results were compared with the analytical solution which was obtained by Özşahin (2013). The finite element model of the problem is given in Figure 2, and the stress distribution obtaining as a result of analysis is given in Figure 4. Some of the results obtained from the solution of the continuous contact problems for the various dimensionless quantities such as the μ_2 / μ_1, a / h, (c-b) / h, Q / P and (b-a) /h by using the analytical and finite element solution are presented in Figures 5-7 and in Tables 1 and 2 by being compared. The initial separation point between the homogenous layer and the elastic half-plane was determined and the initial separation zone was investigated. The contact stress is presented as σy_1 (x, -h) / P /h. In addition, the distance (b-a) / h that end the interaction of the blocks was investigated and accepted as Q / $h \geq P$ / h.

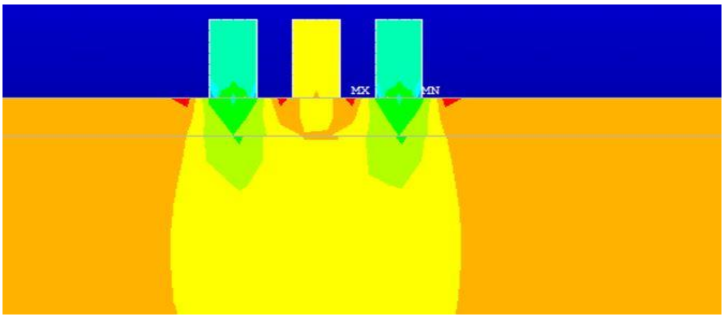

Figure 4. Stress distributions after analysis ($\mu_2 / \mu_1 = 2.75$, $(b-a)/h = 0.5$, $a/h = 0.25$, $(c-b)/h = 0.5$)

Table 1. Variation of the distance depending on the load ratio where the interaction ends between the two blocks which is on the interface of homogeneous layer and elastic semi-infinite plane

			Block I			
		$\lambda_{cr\ right}$			$(\chi_{cr\ right}$-a)/h	
	Analytical	FEM	Error (%)	Analytical	FEM	Error (%)
Q=P (b-a)/h=10.5585	90.9406	89.8957	1.148	2.050	2.050	0
Q=2P (b-a)/h=9.5874	90.4543	89.1186	1.476	2.050	2.050	0
Q=4P (b-a)/h=8.6032	89.0384	86.4155	3.035	2.050	2.050	0
			Block II			
		$\lambda_{cr\ right} = \lambda_{cr\ left}$			(b - $\chi_{cr\ left}$)/h=($\chi_{cr\ right}$-c)/h	
	Analytical	FEM	Error (%)	Analytical	FEM	Error (%)
Q=P (b-a)/h=10.5585	90.8533	89.7666	1.196	2.0085	2.0585	2.489
Q=2P (b-a)/h=9.5874	45.4578	44.9115	1.201	2.0374	2.0566	0.942
Q=4P (b-a)/h=8.6032	22.7580	22.3863	1.633	2.0032	2.0532	2.496

Table 1 shows the critical values of the distance between the blocks obtained by the analytical and finite element method for different states of the (Q/P) load ratio for dimensionless sizes μ_2/μ_1, a/h, $((c-b)/h)$. It is understood that the blocks do not work together in case of higher values than the critical value. Additionally, these tables show the values of the load factor (λ_{cr}) causing the separation between the homogenous layer and the elastic half-plane. $\sigma_{x_1}(x,-h)h/P$ for $\lambda=\lambda_{cr}$ is zero. Contact between the block and the homogeneous layer is continuous. When Table 1 is examined, it is seen that initial separation loads and distances obtained by the finite element method and initial separation loads and distances obtained by analytical solutions are compatible to each other.

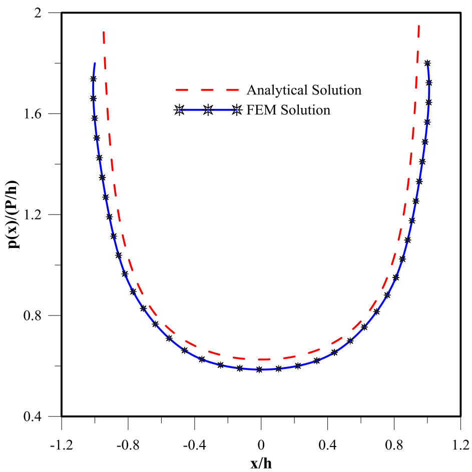

Figure 5a. Stress distribution under Block I ($\mu_2/\mu_1=2.75$, Q=2P, $a/h=0.25$, h=1, $(c-b)/h=0.5$)

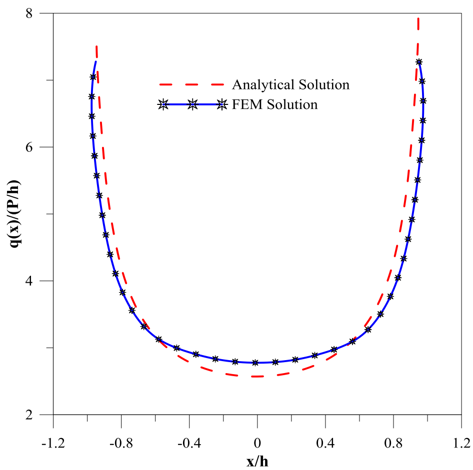

Figure 5b. Stress distribution under Block II ($\mu_2/\mu_1=2.75$, Q=2P, $a/h=0.25$, h=1, $(c-b)/h=0.5$)

The results of contact stresses for the load condition Q = 2P for the same material constants and for the same block widths in Block I and Block II obtained by the analytical method and finite element method were compared in Figures 5(a-b), respectively. When the graphs are examined, it is seen that the analytical results are very close to the results obtained by the finite element method.

The results belonging to the same material constants for the load condition Q = P, Q = 2P and Q = 10P respectively and dimensionless contact stresses along the x-axis between the homogeneous layer and the elastic half-plane for the same block widths which were obtained by the analytical method and finite element method were compared in Figures 6-8. When the graphs are examined, it is observed that the greatest stresses occurred in the bottom of the blocks. It is seen that as the Q / P ratio increases, the critical load factor and initial separation distance decrease as well. Analytical results seem to be very close to the results that were obtained by the finite element method.

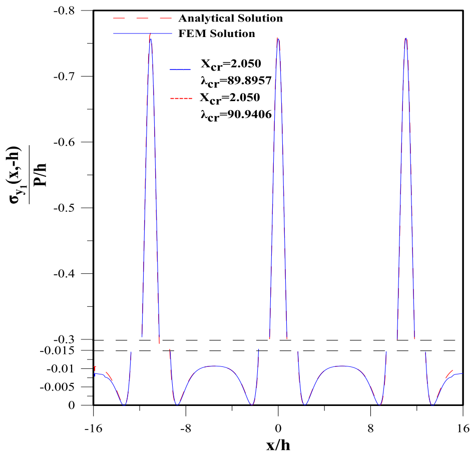

Figure 6. $\sigma_{y_1}(x,0)$ Stress distribution between homogenous layer and elastic plane ($\mu_2/\mu_1 = 2.75$, Q=P, $a/h = 0.25$, h=1, $(c-b)/h = 0.5$)

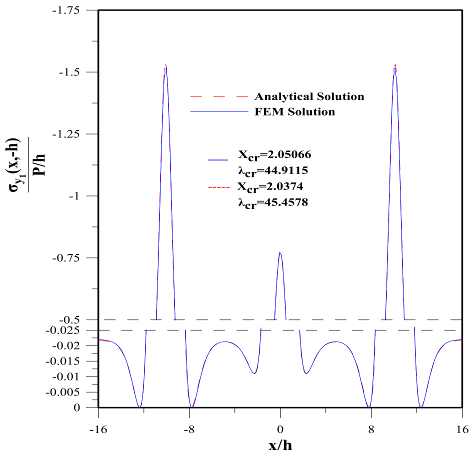

Figure 7. $\sigma_{y_1}(x,0)$ Stress distribution between homogenous layer and elastic plane ($\mu_2/\mu_1 = 2.75$, Q=2P, $a/h = 0.25$, h=1, $(c-b)/h = 0.5$)

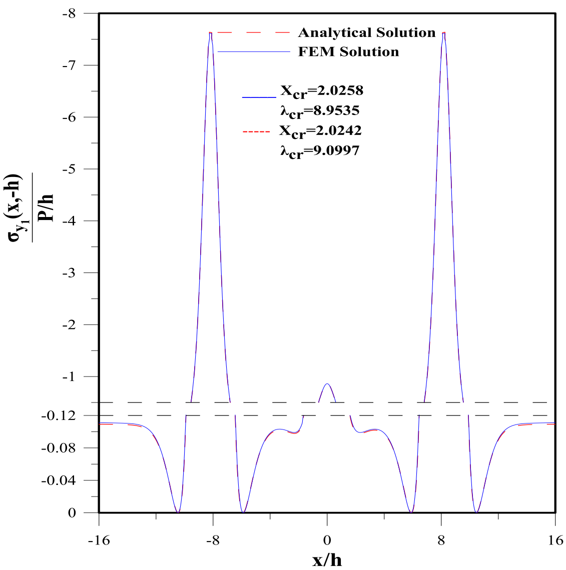

Figure 8. $\sigma_{y_1}(x,0)$ Stress distribution between homogenous layer and elastic plane ($\mu_2/\mu_1 = 2.75$, Q=10P, $a/h = 0.25$, h=1, $(c-b)/h = 0.5$)

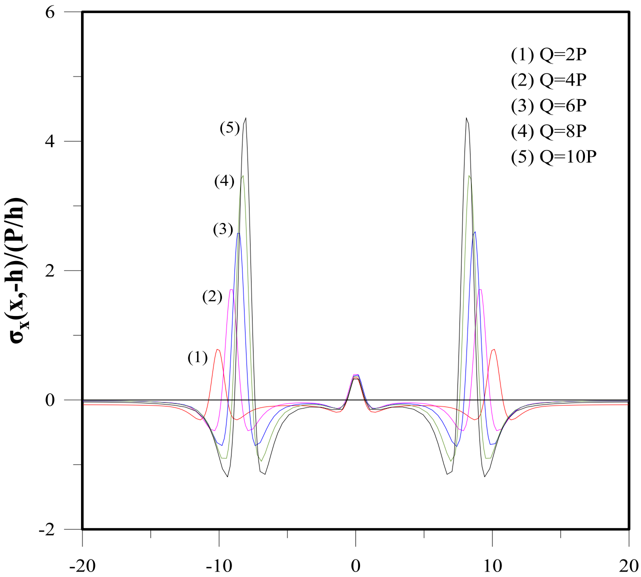

Figure 9. Stress distributions $\sigma_{x_1}(x,0)$ along the axis of layer according to load condition

The variation of stress σ_{x_1} in Figure 9 which occurs along the x-axis between the homogeneous layer and the elastic half-plane for the same material constants and same block widths according to the load ratio were obtained using the finite element method. As the Q / P ratio increases, the values of dimensionless normal stress between the homogeneous layer and the elastic plane which are calculated on pressure zones increases. The compressive stresses occur within the distance between the beginning of the x-axis and Block I, somewhere between the blocks, and in the point immediately after the Block II, and tensile stresses occur at the bottom of the blocks, and these stresses have the greatest values under load.

In case of discontinuous contact, the starting and ending point of the separation between the homogeneous layer and the elastic semi-infinite plane, and the results which was obtained by the finite element method and the analytical solution and belonging to the variation of separation point size depending on the load ratio between layers, are given in Table 2. As the Q / P ratio increases, it is seen that the separation length increases.

Table 2. In case of discontinuous contact, the starting and ending point of the separation depending on the load ratio between the homogeneous layer and the elastic half-plane (μ_2/μ_1 = 0.36, a/h = 0.125, $(b-a)/h$ = 0.5, $(c-b)/h$ = 0.5, λ = 75 > λcr).

Q	d/h			e/h			(d-e)/h		
	Analytical	FEM	Error(%)	Analytical	FEM	Error (%)	Analytical	FEM	Error (%)
Q=2P	3.634	3.764	3.45	6.085	6.253	2.69	2.451	2.489	1.54
Q=3P	3.396	3.524	3.63	7.245	7.513	3.57	3.849	3.989	3.51
Q=4P	3.27	3.374	3.09	8.153	8.443	3.43	4.883	5.069	3.67

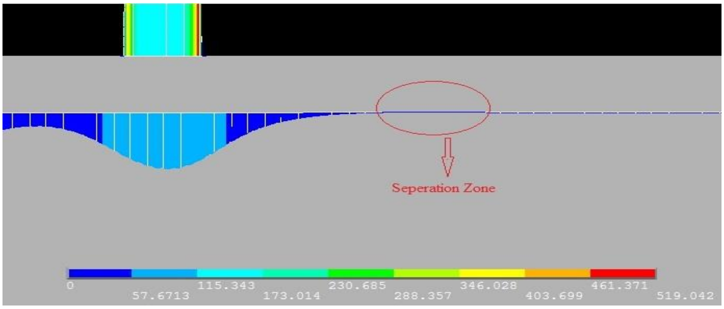

Figure 10. Contact stress distribution and separation zone between homogeneous layer and elastic half-plane in case of discontinuous contact ($Q = 2P$, $a/h = 0.5$, $(b - a)/h = 2$, $(c - b)/h = 1$, $\lambda = 100 > \lambda cr$).

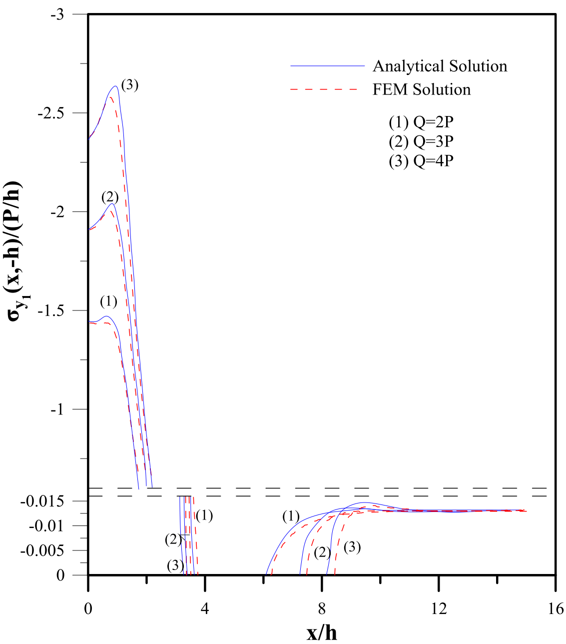

Figure 11. Contact stress distribution between homogeneous layer and elastic half-plane in case of discontinuous contact ($\mu_2/\mu_1 = 0.36$, $a/h = 0.125$, $(b - a)/h = 0.5$, $(c - b)/h = 0.5$, $\lambda = 75 > \lambda cr$).

Figure 10 shows the contact stress distribution and separation zone between the homogeneous layer and the elastic half-plane in the case of discontinuous contact as a result of the finite element analysis with ANSYS software. The stress distributions σ_{y_1} between the homogeneous layer and the elastic half-plane obtained by the analytical method and the finite element method are given in Figure 11 for different load ratios in the case of discontinuous contact. When examining the Figure 11, it is seen that as the Q / P ratio increases, contact stress distribution and separation distance increase. Normalized stresses for the discontinuous contact state indicate three different zones between the homogeneous layer and the elastic semi-infinite plane. These zones are the continuous contact zone where the effect of Q / h and P / h which are the continuous contact zone, separation zone and external loads reduces.

In case of discontinuous contact, the starting and ending point of the separation between the homogeneous layer and the elastic semi-infinite plane interface, and the results which was obtained by the finite element method and the analytical solution and belonging to the variation of separation point size depending on the ratio of the homogeneous layer and elastic plane shear modulus, are given in Table 3. As the shear modulus ratio μ_2 / μ_1 increases, it is seen that the separation approaches the blocks and the separation length increases.

Table 3. In case of discontinuous contact, the starting and ending point of the separation depending on depending on the ratio of the homogeneous layer and elastic plane shear modulus. ($Q = 2P$, $a/h = 0.5$, $(b - a)/h = 2$, $(c - b)/h = 1$, $\lambda = 100 > \lambda$cr).

(μ_2/μ_1)	d/h			e/h			(d-e)/h		
	Analytical	FEM	Error(%)	Analytical	FEM	Error(%)	Analytical	FEM	Error(%)
0.36	6.498	6.643	2.19	7.612	7.753	1.82	1.114	1.109	0.37
0.61	5.869	6.013	2.41	7.299	7.333	0.47	1.43	1.319	7.7
1.65	5.175	5.083	1.76	7.003	7.003	0.007	1.828	1.919	4.77

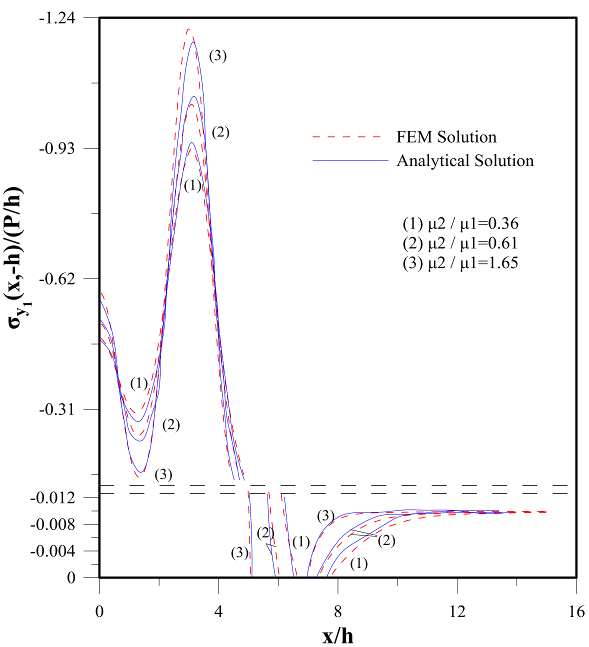

Figure 12. Contact stress distribution between homogeneous layer and elastic half-plane in case of discontinuous contact ($Q = 2$, $a/h = 0.5$, $(b - a)/h = 2$, $(c - b)/h = 1$, $\lambda = 100 > \lambda$cr).

The variations of the stress distributions σ_{y_1} between the homogeneous layer and the elastic half-plane depending on the shear modulus are given in Figure 12 in the case of discontinuous contact (λ> λcr). If the elastic half-plane is harder than the homogenous layer, the separation zone size increases. In this case, the peak value of contact stresses also increases. When Figures 11-12 are examined, it is seen that the results obtained by the finite element method are very compatible with the analytical results.

7. CONCLUSIONS

The continuous and discontinuous contact problem of a homogeneous layer loaded with three rigid flat blocks and resting on the elastic half plane was solved by using finite element method in this study. The effects of the parameters such as load ratios, distances between blocks and shear modulus ratios of homogeneous layer and semi-infinite plane, on the contact zones, initial separation loads and distances, distances where block interactions end, and contact stress distributions were determined in the study by using finite element method (FEM). The results that were obtained were compared with the analytical solution in the literature.

When the results are scrutinized, it is seen that contact stresses and normal stresses obtained by using ANSYS software provide boundary conditions and analytical results. When compared the results obtained with ANSYS software for contact zones with analytical results the error rates were at an acceptable level.

It is known that analytical solution requires complex and long mathematical calculations and it takes a long time. This is a disadvantage for solving problems. However, the Finite Element Method (FEM) provides a quick solution as well as it is practical. In the light of the results that were obtained, it is seen that the results of FEM analysis performed by ANSYS software are very compatible with analytical solutions. For this reason, it can be said that the finite element method can be an alternative to the analytical solution for the solution of the continuous and discontinuous contact problems.

8. NOMENCLATURE

P: Compressive load per unit thickness in z direction on Block I, (N/m)
Q: Compressive load per unit thickness in z direction on Block II and Block III, (N/m)
h: Thickness of the layer, (m)
λ: Load factor
u: x-component of the displacement, (m)
v: y-component of the displacement, (m)
ρ_k: Mass density, (kg/m3)
g: Gravity acceleration, (m/sn2)
μ: Shear modulus, (Pa)
κ: Elastic constant
γ: Poisson's ratio
$(c-b)$: Width of Block II and Block III,(m)
a: Half width of Block I, (m)
$P(x)$: Contact pressure under Block I,(Pa)
$Q(x)$: Contact pressure under Block II and Block III,(Pa)
$(e-d)$: Separation length, (m).

REFERENCES

[1] Hertz H., (1895) Gessammelte Worke. Leipzig, Germany.
[2] Sneddon I.N., (1972) The Use of Integral Transforms, McGraw-Hill, New York.
[3] Adıyaman G., Birinci A., (2013) İki Çeyrek Düzlem Üzerine Oturan Elastik Bir Tabakanın Sürtünmesiz ve Ayrılmalı Temas Problemi, *XVIII. Ulusal Mekanik Kongresi*, Manisa.
[4] Öner E., (2011) The continuous contact problem for two elastic layers loaded by means of a rigid circular punch and resting on an elastic half infinite plane, *A Master Thesis, Institute of Natural Sciences Karadeniz Technical University*, Trabzon.

[5] Ozsahin T.S. and Taskıner O., (2013) Contact Problem for an Elastic Layer on an Elastic Half Plane Loaded by Means of Three Rigid Flat Punches, *Mathematical Problems in Engineering*, Article ID 137427, 14 pages.

[6] Bora P., (2016) The contact problem for two elastic layers loaded by means of two rigid rectangle blocks and resting on an elastic half infinite plane, *A Phd Thesis, Institute of Natural Sciences Karadeniz Technical University*, Trabzon.

[7] Ueda S. and Mukai T., (2002) The Surface Crack Problem for A Layered Elastic Medium with A Functionally Graded Nonhomogeneous Interface, *JSME International Journal Series a Solid Mechanics and Material Engineering*, vol. 45, no. 3, pp. 371-378.

[8] Matysiak S.J., (2003) Edge Crack in An Elastic Layer Resting on Winkler Foundation, *Engineering Fracture Mechanics*, vol. 70, no. 17, pp. 2353-2361.

[9] Dong C.Y., Lo S.Y. and Cheung Y.K., (2004) Numerical Solution for Elastic Half Plane Inclusion Problems by Different Integral Equation Approaches, *Engineering Analysis with Boundary Elements*, vol. 28, pp. 123-130.

[10] Elsharkawy A.A., (1999) Effect of Friction on Subsurface Stresses in Sliding Line Contact of Multilayered Elastic Solids, *International Journal of Solids and Structures*, vol. 36, pp. 3903-3915.

[11] Giannakopoulos A.E. and Pallot P., (2000) Two-Dimensional Contact Analysis of Elastic Graded Materials, *Journal of the Mechanics and Physics of Solids*, vol. 48, pp.1597-1631.

[12] Çömez İ., (2009) Receding contact problem of two elastic layers supported by two elastic quarter planes, *A Phd Thesis, Institute of Natural Sciences Karadeniz Technical University*, Trabzon.

[13] Keer L.M., Dundurs J. and Tasi K.C., (1972) Problems Involving a Receding Contact Between a Layer and a Half-Space, *Journal of Applied Mechanics*, vol. 39, pp.1115–1120.

[14] Kahya V., Ozsahin T.S., Birinci A. and Erdol R., (2007) A Receding Contact Problem for An Anisotropic Elastic Medium Consisting of A Layer And A Half Plane, *International Journal of Solids and Structures*, vol. 44, no. 17, pp.5695–5710.

[15] Adibelli H., Çömez İ. and Erdöl R., (2013) Receding Contact Problem for A Coated Layer And A Half-Plane Loaded By A Rigid Cylindrical Stamp, *Archives of Mechanics*, vol. 65, pp.219-236.

[16] Yan J. and Mi C., (2017) On the Receding Contact between An Inhomogeneously Coated Elastic Layer and A Homogeneous Half-Plane, *Mechanics of Materials*, vol. 112, pp. 18-27.

[17] Yaylaci M., Oner E. and Birinci A., (2014) Comparison Between Analytical and ANSYS Calculations for A Receding Contact Problem, *Journal of Engineering and Mechanics*, vol. 140, no. 9, 04014070.

[18] Chan S.K. and Tuba I. S., (1971) A Finite Element Method for Contact Problems of Solid Bodies—Part I. Theory and Validation, *International Journal of Mechanical Sciences*, vol. 13, pp. 615-625.

[19] Klarbring A., (1986) A Mathematical Programming Approach to Three-Dimensional Contact Problems with Friction, *Computer Methods in Applied Mechanics and Engineering*, vol. 58, no. 2, pp.175-200.

[20] Bostan V. and Han W., (2006) A Posteriori Error Analysis for Finite Element Solutions of A Frictional Contact Problem, *Computer Methods in Applied Mechanics and Engineering*, vol. 195, no. 9-12, pp. 1252–1274.

[21] Roncevic B. and Siminiati D., (2010) Two Dimensional Receding Contact Problem Analysis with NX-NASTRAN, *Advanced Engineering*, vol. 4, pp. 1846-5900.

[22] Adiyaman G., Yaylaci M. and Birinci A., (2015) Analytical and Finite Element Solution of a Receding Contact Problem, *Structural Engineering And Mechanics*, vol. 54, no. 1, pp.69-85.

[23] Yaylacı M., (2017) Comparıson Between Numerıcal and Analytıcal Solutions for the Receding Contact Problem, *Sigma Journal of Engineering and Natural Sciences*, vol. 35, no. 2, pp.333-346.

[24] Oner E., Yaylacı M. and Birinci A., (2015) Analytical solution of a contact problem and comparison with the results from FEM, *Structural Engineering and Mechanics*, vol. 54, no. 4.

[25] Kaya Y., Polat A. and Özşahin T.Ş., Analysis Of Continuous Contact Problem Of Homogeneous Plate Bonded A Rigid Support By Using Finite Element Method, *2nd International Conference On Advanced Engineering Technologies (ICADET 2017)*, 21-23 October 2017 Bayburt, Turkey.

[26] Birinci A., Adıyaman G., Yaylacı M. and Öner E., (2015) Analysis of Continuous and Discontinuous Cases of a Contact Problem Using Analytical Method and FEM, *Latin American Journal of Solids and Structures*, vol. 12, pp.1771-1789.

[27] Polat A., Kaya Y. and Ozsahin T.S., (2018) Analysis of Frictionless Contact Problem for A Layer on An Elastic Half Plane Using FEM, *Düzce Üniversitesi Bilim ve Teknoloji Dergisi*, vol. 6, no. 2, pp. 357-368.

[28] Polat A., Kaya Y. and Ozsahin T.S., (2018) Analytical solution to continuous contact problem for a functionally graded layer loaded through two dissimilar rigid punches, *Meccanica*, vol. 53, no. 14, pp. 3565-3577.

[29] Erdogan F. and Gupta G., (1972) On The Numerical Solutions of Singular Integral Equations, *Quarterly of Applied Mathematics*, vol. 29, pp. 525-534.

[30] ANSYS, (2015) Swanson Analysis Systems Inc., Houston PA, USA.

[31] Biswas P.K. and Banerjee S., (2013) ANSYS Based FEM Analysis for Three And Four Coil Active Magnetic Bearing-A Comparative Study, *International Journal of Applied Science and Engineering*, vol. 11, no. 3, pp. 277-292.